

Influence of Bridging Ligand Unsaturation on Excited State Behavior in Mono- and Bimetallic Ruthenium(II) Diimine Complexes

Aaron I. Baba, Harry E. Ensley, and Russell H. Schmehl*

Department of Chemistry, Tulane University, New Orleans, Louisiana 70118

Received August 27, 1993[⊗]

The redox and photophysical properties of a series of bis(bipyridine)-bridged bimetallic complexes of the type $[(\text{dmb})_2\text{Ru}(\text{BL})](\text{PF}_6)_2$ and $\{[(\text{dmb})_2\text{Ru}](\text{BL})\}(\text{PF}_6)_4$ ($\text{dmb} = 4,4'$ -dimethyl-2,2'-bipyridine; $\text{BL} = 1,4$ -bis(4'-methyl-2,2'-bipyridin-4-yl)buta-1,3-diene (**bbdb**), 1,4-bis(4'-methyl-2,2'-bipyridin-4-yl)-2-cyclohexene-5,6-dicarboxylic acid diethyl ester (**bchb**), and 1,4-bis(4'-methyl-2,2'-bipyridin-4-yl)benzene (**bphb**)) are reported. Complexes having cyclohexenyl and phenyl bridging ligands have redox and photophysical properties similar to the parent complex of the series, $[(\text{dmb})_3\text{Ru}](\text{PF}_6)_2$. The butadienyl complexes exhibit very weak luminescence and transient absorbance spectra which are indicative of the presence of another excited state. For $[(\text{dmb})_2\text{Ru}(\text{bbdb})](\text{PF}_6)_2$ the room temperature luminescence lifetime differs from the lifetime obtained by transient absorbance and the luminescence and transient absorbance are quenched with different rate constants by a series of triplet quenchers. The results suggest that the complexes of **bbdb** have a second excited state which is populated along with the $^3\text{MLCT}$ state. A comparison of the luminescence behavior of several different bridged complexes with the triplet energies of related aromatic hydrocarbons suggests that the triplet energy of the bridging ligand is relatively unaffected by coordination.

Introduction

Photochemical studies of covalently linked transition metal complex clusters are of interest for a variety of purposes. Such clusters represent model systems for the development of photochemical molecular devices wherein supramolecular assemblies of components perform specific functions following electronic excitation.¹⁻³ In addition photochemically active clusters also provide molecular systems for the study of light induced energy⁴⁻¹² and electron transfer¹³⁻²⁰ reactions, self-exchange processes, and exciton migration. Ligands which bridge independent metal centers having isolated chromophores in such systems can play a critical role in influencing energy and electron transfer processes.⁴ For example, in a bridged bimetallic complex of the type $[\text{L}_2\text{M}(\text{BL})\text{M}'\text{L}'_2]$ ($\text{BL} =$ bridging

ligand) where energy or electron transfer occurs from the $\text{L}_2\text{M}(\text{BL})$ chromophore to the $(\text{BL})\text{M}'\text{L}'_2$ chromophore, the efficiency of the electron/energy transfer is a function of the degree of electronic coupling of the metal centers through the bridging ligand. In complexes having bridging ligands composed of heterocyclic aromatic hydrocarbons, increasing electronic coupling will ultimately lead to a strongly coupled system lacking discrete donor and acceptor centers.³⁹ The coupling is enhanced upon increasing the density of low-lying unoccupied orbitals (i.e. ligand π^* orbitals); unfortunately, the existence of such orbitals is often accompanied by the existence of low-energy ligand localized excited states (Figure 1) that can serve as energy traps to circumvent the desired energy/electron transfer process.

Such intraligand (IL) excited states have been observed in numerous complexes of transition metals.²¹⁻²⁵ The most direct

[⊗] Abstract published in *Advance ACS Abstracts*, February 15, 1995.

- (1) See: Balzani, V.; Scandola, F. *Supramolecular Photochemistry*; Ellis Horwood Ltd.: Chichester, U.K., 1991.
- (2) See: Schneider, H. J.; Duerr, H. *Frontiers in Supramolecular Organic Chemistry and Photochemistry*; VCH: Weinheim, Germany, 1991.
- (3) See: Mirkin, C. A.; Batner, M. A. *Annu. Rev. Phys. Chem.* **1992**, *43*, 719.
- (4) (a) Ryu, C. K.; Schmehl, R. H. *J. Phys. Chem.* **1989**, *93*, 7961. (b) Schmehl, R. H.; Auerbach, R. A.; Wacholtz, W. F. *J. Phys. Chem.* **1988**, *92*, 6202. (c) Wacholtz, W. F.; Auerbach, R. A.; Schmehl, R. H. *Inorg. Chem.* **1987**, *26*, 2989. (d) Schmehl, R. H.; Auerbach, R. A.; Wacholtz, W. F.; Elliott, C. M.; Freitag, R. A.; Merkert, J. W. *Inorg. Chem.* **1986**, *25*, 2440.
- (5) (a) Schanze, K. S.; MacQueen, D. B.; Perkins, T. A.; Cabana, L. A. *Coord. Chem. Rev.* **1993**, *122*, 63. (b) MacQueen, D. B.; Eyler, J. R.; Schanze, K. S. *J. Am. Chem. Soc.* **1992**, *114*, 1897.
- (6) Van Wallendaal, S.; Rillema, D. P. *Coord. Chem. Rev.* **1991**, *111*, 297.
- (7) (a) Jones, W. E., Jr.; Baxter, S. M.; Mecklenburg, S. L.; Erickson, B. W.; Peek, B. M.; Meter, T. J. *NATO ASI Ser., Ser. C* **1992**, *371*, 249. (b) Murtaza, Z.; Zipp, A. P.; Worl, L. A.; Graff, D.; Jones, W. E., Jr.; Bates, W. D.; Meyer, T. J. *J. Am. Chem. Soc.* **1991**, *113*, 5113. (c) Meyer, T. J. *Pure Appl. Chem.* **1990**, *62*, 1003. (d) Tapolsky, G.; Duesing, R.; Meyer, T. J. *Inorg. Chem.* **1990**, *29*, 2285. (e) Boyde, S.; Strouse, G. F.; Jones, W. E., Jr.; Meter, T. J. *J. Am. Chem. Soc.* **1989**, *111*, 7448.
- (8) (a) Endicott, J. F.; Lessard, R. B.; Lei, Y.; Ryu, C. K. *NATO ASI Ser. C* **1987**, *214*, 167. (b) Endicott, J. F.; Tamilarasan, R.; Brubaker, G. R. *J. Am. Chem. Soc.* **1986**, *108*, 5193. (c) Lei, Y.; Buranda, T.; Endicott, J. F. *J. Am. Chem. Soc.* **1990**, *112*, 8820.
- (9) (a) Denti, G.; Campagna, S.; Serroni, S.; Ciano, M.; Balzani, V. *J. Am. Chem. Soc.* **1992**, *114*, 2944. (b) DeCola, L.; Barigelletti, F.; Balzani, V.; Belsler, P.; von Zelewski, A.; Seel, C.; Frank, M.; Voegtle, F. *Coord. Chem. Rev.* **1991**, *111*, 255. (c) Denti, G.; Serroni, S.; Campagna, S.; Ricevuto, V.; Balzani, V. *Coord. Chem. Rev.* **1991**, *111*, 227. (d) Armaroli, N.; Balzani, V.; Barigelletti, F.; DeCola, L.; Sauvage, J.-P.; Hemmert, C. *J. Am. Chem. Soc.* **1991**, *113*, 4033. (e) DeCola, L.; Barigelletti, F.; Balzani, V.; Hage, R.; Haasnoot, J. G. Reedijk, J.; Vos, J. G. *Chem. Phys. Lett.* **1991**, *178*, 491.
- (10) (a) Bignozzi, C. A.; Argazzi, R.; Garcia, C. G.; Scandola, F.; Schoonover, J. R.; Meyer, T. J. *J. Am. Chem. Soc.* **1992**, *114*, 9727. (b) Bignozzi, C. A.; Bortolini, O.; Chiorboli, C.; Indelli, M. T.; Rampi, M. A.; Scandola, F. *Inorg. Chem.* **1992**, *31*, 172. (c) Chiorboli, C.; Bignozzi, C. A.; Indelli, M. T.; Rampi, M. A.; Scandola, F. *Coord. Chem. Rev.* **1991**, *111*, 267. (d) Bignozzi, C. A.; Argazzi, R.; Chiorboli, C.; Roffia, S.; Scandola, F. *Coord. Chem. Rev.* **1991**, *111*, 261. (e) Bignozzi, C. A.; Indelli, M. T.; Scandola, F. *J. Am. Chem. Soc.* **1989**, *111*, 5192.
- (11) (a) Petersen, J. D.; Morgan, L. W.; Hsu, I.; Billadeau, M. A.; Ronco, S. E. *Coord. Chem. Rev.* **1991**, *111*, 319. (b) MacQueen, D. B.; Petersen, J. D. *Coord. Chem. Rev.* **1990**, *97*, 249. (c) Petersen, J. D. *NATO ASI Ser., Ser. C* **1987**, *214*, 135. (d) Moore, K. J.; Lee, L.; Figard, J. E.; Gelroth, J. A.; Stinson, A. J.; Wohlers, H. D.; Petersen, J. D. *J. Am. Chem. Soc.* **1983**, *105*, 2274.
- (12) (a) Furue, M.; Naok, M.; Kanematsu, Y.; Kushida, T.; Kamachi, M. *Coord. Chem. Rev.* **1991**, *111*, 221. (b) Furue, M.; Yoshidzumi, T.; Kinoshita, S.; Kushida, T.; Nozakura, S.; Kamachi, M. *Bull. Chem. Soc. Jpn.* **1991**, *64*, 1632. (c) Furue, M.; Kinoshita, S.; Kushida, T. *Chem. Lett.* **1987**, 2355.

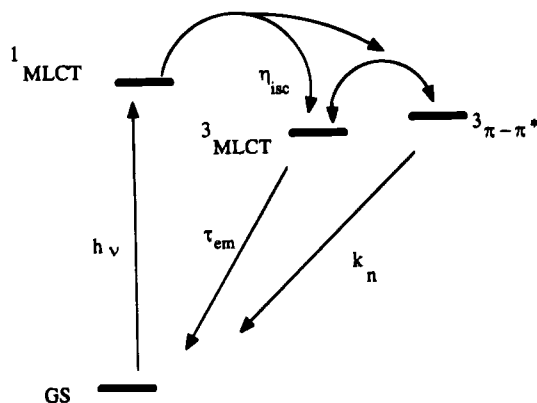
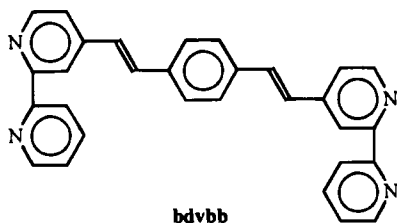


Figure 1. Relative energy level diagram of excited states observed and excited state decay processes of Ru(II) diimine complexes.

indication of the involvement of ^3IL states, structured phosphorescence, occurs in Re(I) diimine complexes. In the 1970's Wrighton and co-workers reported ligand-localized phosphorescence for pyridyl ketone complexes in room temperature solutions.²⁵ Recently Demas⁴² and Rillema⁴³ have observed both intraligand phosphorescence and charge transfer emission in other Re(I) complexes. Luminescence from both ^3IL and $^3\text{MLCT}$ states has been observed in mixed phenanthroline-triphenylphosphine complexes of Cu(I).^{23c} The two emitting states were found to be nonequilibrated, and no direct evidence was obtained for internal conversion between the two states. We have previously found the complex $[(\text{CO})_3(\text{CH}_3\text{CN})\text{Re}(\text{bdvbb})\text{Re}(\text{CH}_3\text{CN})(\text{CO})_3]^{2+}$ (**bdvbb** shown) exhibits both



structured ^3IL phosphorescence in room temperature solutions and a unique transient absorbance with a long wavelength absorption which is different than the absorbance of Re(I) diimine complexes having $^3\text{MLCT}$ states.^{22a} In Ru(II) com-

plexes of **bdvbb**, a long wavelength transient absorbance is observed which has a lifetime that differs from that of the $^3\text{-MLCT}$ luminescence, suggesting the presence of two nonequilibrated excited states.^{22b} In addition, the transient absorbance (TA) is quenched at different rates than the luminescence by a series of triplet quenchers. The free energy dependence of the TA quenching suggests the energy of the state quenched is between 14 100 and 14 500 cm^{-1} , which is close to the intraligand state energy observed in Re(I) complexes. Though only a few systems exhibiting coexistence of IL and MLCT states have been examined in detail, a common feature is that internal conversion between the two emitting states is slow relative to other relaxation processes. Excited state lifetimes of the two states vary by orders of magnitude in some cases, indicating the two states are not in equilibrium.

The results presented here expand upon earlier work to illustrate the correlation between triplet energies of aromatic hydrocarbons and the photophysical behavior of complexes containing structurally related aza derivatives of the hydrocarbons as ligands. The bridging ligands reported here are shown in Chart 1, and the complexes studied are $[(\text{dmb})_2\text{Ru}(\text{BL})](\text{PF}_6)_2$ and $\{[(\text{dmb})_2\text{Ru}]_2(\text{BL})\}(\text{PF}_6)_4$. The synthesis of the ligands and complexes are reported as well as electrochemical and spectral characterization. The photophysical behavior of the complexes illustrates the influence of IL excited states on charge transfer luminescence and the link between ligand ^3IL state energies and triplet energies of closely related hydrocarbons.

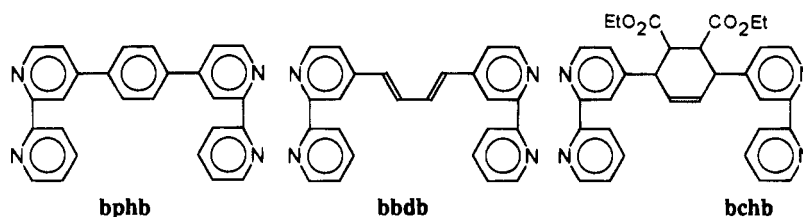
Experimental Section

General Methods. Melting points (uncorrected) were obtained using an Electrothermal 9100 apparatus. All reagents were used as received unless otherwise specified. 4,4'-Dimethyl-2,2'-bipyridine was recrystal-

- (13) (a) Closs, G. L.; Johnson, M. D.; Miller, J. R.; Piotrowiak, P. *J. Am. Chem. Soc.* **1989**, *111* (10), 3751-3. (b) Closs, G. L.; Miller, J. R. *Science* **1988**, *240* (4851), 440-7. (c) Closs, G. L.; Piotrowiak, P.; MacInnis, J. M.; Fleming, G. R. *J. Am. Chem. Soc.* **1988**, *110* (8), 2652-3. (d) Liang, N.; Miller, J. R.; Closs, G. L. *J. Am. Chem. Soc.* **1990**, *112* (13), 5353. (e) Liang, N.; Miller, J. R.; Closs, G. L. *J. Am. Chem. Soc.* **1989**, *111*, (23), 8740.
- (14) McLendon, G.; Conklin, K. J.; Corvan, R.; Johansson, K.; Magner, E.; O'Neil, M.; Pardue, K.; Rogalski, J. S.; Whitten, D. *Photochem. Energy Convers., Proc. Int. Conf. Photochem. Convers. Storage Solar Energy*, 7th; Meeting Date 1988; Norris, James, R., Jr., Meisel, D., Eds.; Elsevier: New York, 1989, pp 47-59. (b) McLendon, G. *Acc. Chem. Res.* **1988**, *21* (4), 160-7. (c) McGuire, M.; McLendon, G. *J. Phys. Chem.* **1986**, *90* (12), 2549-51.
- (15) (a) Wasielewski, M. R.; Johnson, D. G.; Svec, W. A.; Kersey, K. M.; Minsek, D. W. *J. Am. Chem. Soc.* **1988**, *110* (21), 7219-21. (b) Schmidt, J. A.; McIntosh, A. R.; Weedon, A. C.; Bolton, J. R.; Connolly, J. S.; Hurley, J. K.; Wasielewski, M. R. *J. Am. Chem. Soc.* **1988**, *110* (6), 1733-40. (c) Wasielewski, M.; Niemczyk, M. P.; Johnson, D. G.; Svec, W. A.; Minsek, D. W. *Tetrahedron* **1989**, *45*, 4785-4806.
- (16) (a) Miller, J. R. *NATO ASI Ser., Ser. C* **1987**, *214*, 241-54. (b) Miller, J. R. *New J. Chem.* **1987**, *11* (2), 83-9.
- (17) (a) Cabana, L. A.; Schanze, K. S. *Adv. Chem. Ser.* **1989**, No. 226, 101-24. (b) Perkins, T. A.; Hauser, B. T.; Eyley, J. R.; Schanze, K. S. *J. Phys. Chem.* **1990**, *94* (25), 8745-8. (c) Schanze, K. S.; Cabana, L. A. *J. Phys. Chem.* **1990**, *94* (7), 2740-3. (d) Schanze, K. S.; Sauer, K. J. *J. Am. Chem. Soc.* **1988**, *110* (4), 1180-6.

- (18) (a) Younathan, J. N.; Jones, W. E., Jr.; Meyer, T. J. *J. Phys. Chem.* **1991**, *95* (1), 488. (b) Meyer, T. J. *Pure Appl. Chem.* **1990**, *62* (6), 1003-9. (c) Tapolsky, G.; Duesing, R.; Meyer, T. J. *Inorg. Chem.* **1990**, *29* (12), 2285-97. (d) Duesing, R.; Tapolsky, G.; Meyer, T. J. *J. Am. Chem. Soc.* **1990**, *112* (13), 5378-9. (e) Tapolsky, G.; Duesing, R.; Meyer, T. J. *J. Phys. Chem.* **1989**, *93* (10), 3995-7. (f) Chen, P.; Duesing, R.; Tapolsky, G.; Meyer, T. J. *J. Am. Chem. Soc.* **1989**, *111* (21), 8305-6. (g) Chen, P.; Danielson, E.; Meyer, T. J. *J. Phys. Chem.* **1988**, *92* (13), 3708-11.
- (19) (a) Cooley, L. F.; Headford, C. E. L.; Elliott, C. M.; Kelley, D. F. *J. Am. Chem. Soc.* **1988**, *110* (20), 6673-82. (b) Danielson, E.; Elliott, C. M.; Merkert, J. W.; Meyer, T. J. *J. Am. Chem. Soc.* **1987**, *109* (8), 2519-20. (c) Elliott, C. M.; Freitag, R. A.; Blaney, D. D. *J. Am. Chem. Soc.* **1985**, *107*, 4647-4654. (d) Ryu, C. K.; Wang, R.; Schmehl, R. H.; Ferrere, S.; Ludwickow, M.; Merkert, J. W.; Headford, C. E. L.; Elliott, C. M. *J. Am. Chem. Soc.* **1992**, *114*, 430. (e) Yonemoto, E. H.; Riley, R. L.; Kim, Y. I.; Atherton, S. J.; Schmehl, R. H.; Mallouk, T. E. *J. Am. Chem. Soc.* **1992**, *114*, 8081.
- (20) (a) Antolovich, M.; Keyte, P. J.; Oliver, A. M.; Paddon-Row, M. N.; Kroon, J.; Verhoeven, J. W.; Jonker, S. A.; Warman, J. M. *J. Phys. Chem.* **1991**, *95* (5), 1933-41. (b) Warman, J. M.; Smit, K. J.; de Haas, M. P.; Jonker, S. A.; Paddon-Row, M. N.; Oliver, A. M.; Kroon, J.; Oevering, H.; Verhoeven, J. W. *J. Phys. Chem.* **1991**, *95* (5), 1979-87. (c) Vassilian, A.; Wishart, J. F.; van Hemelryck, B.; Schwarz, H.; Isied, S. S. *J. Am. Chem. Soc.* **1990**, *112*, (20), 7278-86. (d) Isied, S. S. *Adv. Chem. Ser.* **1989**, No. 226, 91-100. (e) Gust, D.; Moore, T. A. *Science* **1989**, *244* (4900), 35-41. (f) Gust, D.; Moore, T. A.; Moore, A. L.; Makings, L. R.; Seely, G. R.; Ma, X.; Trier, T. T.; Gao, F. *J. Am. Chem. Soc.* **1988**, *110* (22), 7567-9.
- (21) (a) King, K. A.; Watts, R. J. *J. Am. Chem. Soc.* **1987**, *109*, 1589. (b) Watts, R. J.; Crosby, G. A.; Sansregret, J. L. *Inorg. Chem.* **1972**, *11*, 1474.
- (22) (a) Shaw, J. R.; Schmehl, R. H. *J. Am. Chem. Soc.* **1991**, *113*, 389. (b) Shaw, J. R.; Webb, R. T.; Schmehl, R. H. *J. Am. Chem. Soc.* **1990**, *112*, 1117. (c) Belsor, P.; von Zelewsky, A.; Juris, A.; Barigelletti, F.; Tucci, A.; Balzani, V. *Chem. Phys. Lett.* **1982**, *89*, 101.
- (23) (a) Ratliff, K. S.; DeLaet, D. L.; Gao, J.; Fanwick, P. E.; Kubiak, C. P. *Inorg. Chem.* **1990**, *29*, 4022. (b) Rader, R. A.; McMillin, D. R.; Buckner, M. T.; Matthews, T. G.; Casadonte, D. J.; Lengel, R. K.; Whittaker, S. B.; Darmon, L. M.; Lytle, F. E. *J. Am. Chem. Soc.* **1981**, *103*, 5906. (c) Buckner, M. T.; Matthews, T. G.; Lytle, F. E.; McMillin, D. R. *J. Am. Chem. Soc.* **1979**, *101*, 5846. (d) Casadonte, D. J.; McMillin, D. R. *J. Am. Chem. Soc.* **1987**, *109*, 331.

Chart 1



lized from THF before use. NMR spectra were recorded on either a GE 400 or Bruker AC200 spectrometer. Mass spectra at high resolution and FAB mass spectra were obtained using a Kratos Profile spectrometer. UV-vis spectra were run on a HP8452 diode array spectrophotometer. Luminescence spectra were obtained with a SPEX Fluorolog equipped with a 450 W Xe arc lamp, thermostated cell holder, and thermoelectrically cooled PMT. Spectra were corrected for photomultiplier response. Luminescence lifetimes, quantum yields, and transient absorption spectra^{22b} were measured using apparatus previously described. The reference for quantum yield measurements was [Ru(bpy)₃](PF₆)₂ in acetonitrile ($\phi_{\text{ref}} = 0.086$);³⁸ quantum yields were corrected for solvent refractive index differences. Some of the transient absorbance measurements were made using facilities at the center for Fast Kinetics Research at the University of Texas.

Cyclic voltammograms were obtained with a Princeton Applied Research Model 173 potentiostat, Model 175 universal programmer, and Model 176 current follower. Voltammograms were measured using either Pt or glassy carbon working electrodes, a Pt coil counter electrode, and a Ag/AgCl pseudo-reference electrode in acetonitrile freshly distilled from CaH₂ under N₂. Differential pulse polarograms were recorded using a PAR Model 384B polarographic analyzer. Ferrocene was added as an internal reference in all experiments; potentials are reported relative to the saturated SCE electrode.

Ligand Preparations. All reactions were carried out under a nitrogen atmosphere unless specified otherwise. Silica gel used in chromatography was 230–400 mesh.

1,4-Bis(4'-methyl-2,2'-bipyridin-4-yl)buta-1,3-diene, bbdb. To a clean, dry, one-necked round-bottomed flask 10 g (0.054 mol) of 4,4'-dimethyl-2,2'-bipyridine (dmb, Reilly Tar and Chemical), 11.53 g (0.064 mol) of *N*-bromosuccinimide (Aldrich), and 1.1 g of AIBN (Kodak) were refluxed in 200 mL of CCl₄ on an oil bath for 3 h. The mixture was cooled to 40 °C, and the precipitated succinimide was removed by vacuum filtration and washed with 50 mL of cold CCl₄. The washings and filtrate were combined and evaporated to dryness on a rotary evaporator. The crude solid was dissolved in benzene (250 mL),

and triphenyl phosphine (14.15 g, 0.054 mol) was added. The mixture was refluxed under N₂ for 12 h, cooled to room temperature, and filtered. The solid phosphonium salt obtained was washed with benzene (50 mL) and ether (50 mL) and dried in vacuo at room temperature.

The phosphonium salt obtained (23.6 g, 0.049 mol) was dissolved in 200 mL of absolute ethanol, and glyoxal trimeric hydrate (1.72 g, 0.0082 mol) in DMSO (25 mL) was added. The mixture was refluxed for 45 min followed by addition of sodium methoxide (5.29 g, 0.097 mol). The solution was refluxed for 12 h, cooled to room temperature, and evaporated to half the original volume. The dark brown solution was treated with 30 mL of HCl (concentrated), and the protonated bipyridinium salts were precipitated by addition of acetone (200 mL). The precipitate was collected by filtration, dissolved in water, and filtered to remove insoluble residue, and the filtrate was treated with saturated Na₂CO₃ to precipitate the butadiene derivative. The solid was collected by filtration, dried under vacuum, and flash chromatographed on silica gel using CHCl₃:EtOAc:Et₃N (4:4:1) as eluent. Yields for the reaction are typically around 25%. Mp: 220 °C. HRMS (*m/z*): 390.18479 (deviation, 0.87 ppm; peaks *m/z* 390, 221, 170). ¹H NMR (400 MHz, CDCl₃): δ 8.60 (d, 2H), 8.56 (d, 2H), 8.43 (d, 2H), 8.23 (d, 2H), 7.29 (m, 4H), 7.15 (d, 2H), 6.75 (m, 2H), 2.43 (s, 6H). MS [*m/z* (M⁺)]: calcd, 390.1839; obsd, 390.1848.

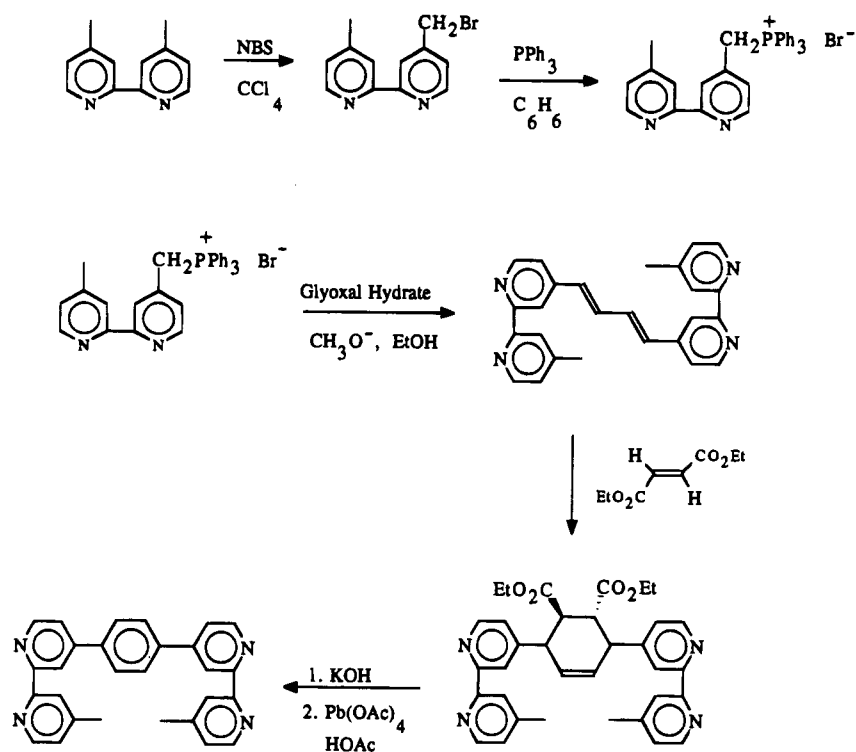
1,4-Bis(4-methyl-2,2'-bipyridin-4-yl)-2-cyclohexene-5,6-dicarboxylic Acid Diethyl Ester, bchb. The butadiene ligand, bbdb (4.04 g, 0.010 mol) was refluxed in diethyl fumarate (4.82 mL, 0.031 mol) for 3.5 h. Excess fumarate was removed by vacuum distillation, and the oily residue was directly loaded on a flash chromatography column of silica gel (230–400 mesh, 6 in. \times 2 in. diameter) and eluted with the 4:4:1 mixture of CHCl₃:EtOAc:Et₃N. The resulting Diels–Alder adduct was recrystallized from methanol. Mp: 135–138 °C. HRMS (*m/z*): calcd, 562.2580; found, 562.2555 (peaks 562, 489, 415). ¹H NMR (CDCl₃): 8.59 (2H, d); 8.54 (2H, d); 8.39 (1H, s); 8.34 (1H, s); 8.23 (2H, s); 7.26 (1H, d); 7.22 (1H, d); 7.13 (2H, s); 6.57 (1H, s); 4.17 (1H, s); 3.90 (4H, d of q); 3.25 (2H, m); 2.59 (2H, s); 2.42 (6H, s); 0.92 (6H, d of t).

1,4-Bis(4-methyl-2,2'-bipyridin-4-yl)-2-cyclohexene-5,6-dicarboxylic Acid. Hydrolysis of the ester with KOH in ethanol yielded the diacid following evaporation of the ethanol, filtration to remove unreacted diester, and precipitation of the acid from water using 0.2 M HCl and acidification to pH 5.5. Yields for conversion of bbdb to the diacid were typically 40–50%. IR (KBr): 1723 cm⁻¹ (ν_{CO}). The diacid was used directly in preparation of bphb, below.

- (24) (a) Ferraudi, G.; Granifo, J. J. *Phys. Chem.* **1985**, *89*, 1206. (b) Schmatz, K.; Muralidharan, S.; Madden, K.; Fessenden, R.; Ferraudi, G. *Inorg. Chim. Acta* **1982**, *64*, L23.
- (25) (a) Fredericks, S. M.; Luong, J. C.; Wrighton, M. S. *J. Am. Chem. Soc.* **1979**, *101*, 7415. (b) Giordano, P. J.; Fredericks, S. M.; Wrighton, M. S.; Morse, D. L. *J. Am. Chem. Soc.* **1978**, *100*, 2257. (c) Pdungsap, L.; Wrighton, M. S. *J. Organomet. Chem.* **1977**, *17*, 337. (d) Juris, A.; Campagna, S.; Bidd, I.; Lehn, J.-M.; Ziessel, R. *Inorg. Chem.* **1988**, *27*, 4007.
- (26) (a) Indelli, M. T.; Scandola, F. *Inorg. Chem.* **1990**, *29*, 3056. (b) Bolletta, F.; Rossi, A.; Barigelletti, F.; Dellonte, S.; Balzani, V. *Gazz. Chim. Ital.* **1991**, *111*, 155.
- (27) (a) Wacholtz, W. F.; Auerbach, R. A.; Schmehl, R. H. *Inorg. Chem.* **1986**, *25*, 227. (b) Wacholtz, W. F.; Auerbach, R. A.; Schmehl, R. H. *Inorg. Chem.* **1987**, *26*, 2989.
- (28) Ciana, L. D.; Hamachi, I.; Meyer, T. J. *J. Org. Chem.* **1989**, *54*, 1731.
- (29) (a) Braunstein, C. H.; Baker, A. D.; Streckas, T. C.; Gafny, H. D. *Inorg. Chem.* **1984**, *23*, 857. (b) Fuchs, Y.; Lofters, S.; Dieeter, T.; Shi, W.; Morgan, R.; Streckas, T. C.; Gafny, H. D.; Baker, A. D. *J. Am. Chem. Soc.* **1987**, *109*, 2691.
- (30) (a) Hunziker, M.; Ludi, A. *J. Am. Chem. Soc.* **1977**, *99*, 7370. (b) Rillema, D. P.; Mack, K. B. *Inorg. Chem.* **1982**, *21*, 3849. (c) Sahai, R.; Morgan, L.; Rillema, D. P. *Inorg. Chem.* **1988**, *27*, 3495.
- (31) Richardson, D. E.; Taube, H. *Inorg. Chem.* **1981**, *20*, 1278.
- (32) Boyde, S.; Strouse, G. F.; Jones, W. E., Jr.; Meyer, T. J. *J. Am. Chem. Soc.* **1990**, *112*, 7395.
- (33) (a) Myer, T. J. *Pure Appl. Chem.* **1986**, *58*, 1576. (b) Caspar, J. V.; Kober, E. M.; Sullivan, B. P.; Meyer, T. J. *J. Am. Chem. Soc.* **1982**, *104*, 630.

- (34) Murov, S. L. *Handbook of Photochemistry*; Dekker: New York, 1973; p 5.
- (35) Sundahl, M.; Wennerstrom, O.; Sandros, K.; Arai, T.; Tokumaru, K. *J. Phys. Chem.* **1990**, *94*, 6731.
- (36) Chattopadhyay, S. K.; Kumar, C. V.; Das, P. K. *J. Photochem.* **1984**, *26*, 39.
- (37) (a) Görner, H. *J. Phys. Chem.* **1989**, *93*, 1826. (b) Elisi, F.; Mazzucato, U.; Görner, H. *J. Photochem.* **1987**, *37*, 87.
- (38) Kawanishi, Y.; Kitamura, N.; Kim, Y.; Tazuke, S. *Riken. Q.* **1984**, *78*, 212.
- (39) Creutz, C. *Progr. Inorg. Chem.* **1983**, *30*, 1.
- (40) Woitellier, S.; Launay, J. P.; Spangler, C. W. *Inorg. Chem.* **1989**, *28*, 758.
- (41) Baba, A. I.; Wang, W.; Kim, W. Y.; Strong, L.; Schmehl, R. H. *Synth. Commun.* **1994**, *24*, 1029.
- (42) (a) Zipp, A.; Sacksteder, L. A.; Streich, J.; Cook, A.; Demas, J. N.; DeGraff, B. A. *Inorg. Chem.* **1993**, *32*, 5629. (b) Sacksteder, L.; Lee, M.; Demas, J. N.; DeGraff, B. A. *J. Am. Chem. Soc.* **1993**, *115*, 8230. (c) Sacksteder, L.; Zipp, A. P.; Brown, E. A.; Streich, J.; Demas, J. N.; DeGraff, B. A. *Inorg. Chem.* **1990**, *29*, 4335.
- (43) Wallace, L.; Rillema, D. P. *Inorg. Chem.* **1993**, *32*, 3836.

Scheme 1



1,4-Bis(4-methyl-2,2'-bipyridin-4'-yl)benzene, bphb. The acid obtained from hydrolysis of **bchb** (1.4 g, 0.0027 mol) and $\text{Pb}(\text{OAc})_4$ was dissolved in 2 mL of acetic acid and heated to reflux on an oil bath for 20 min. To this solution DMF (5 mL) was added, and the solution was refluxed for an additional 3.5 h. The solution was cooled to room temperature and poured into 50 mL of H_2O , made basic by addition of Na_2CO_3 and extracted with CHCl_3 (3×20 mL). The extract was concentrated to 5 mL and loaded onto a flash chromatography column of silica gel and eluted with $\text{CHCl}_3:\text{EtOAc}:\text{Et}_3\text{N}$ (4:4:1). Yield: 0.20 g, 18% after chromatography. Mp: 205–207 °C. HRMS (M^+) (m/z): calcd, 414.1850; found, 414.1840 (peaks 414, 207). ^1H NMR (400 MHz, CDCl_3): 8.75 (d, 2H), 8.70 (s, 2H), 8.6 (d, 2H), 8.30 (s, 2H), 7.89 (s, 4H), 7.6 (d, 2H), 7.15 (d, 2H), 2.42 (s, 6H).

Complex Syntheses. General preparations of the complexes are given below followed by details for individual complexes. Additional FAB mass spectral data is provided as supplementary material.

General Preparation of $[(\text{dmb})_2\text{Ru}(\text{b-b})](\text{PF}_6)_2$. A solution of $[(\text{dmb})_2\text{RuCl}_2]$ (1 equiv) and b-b (10 equiv) in ethanol was refluxed under N_2 for 3–5 h during which time the solution color changed from purple to orange. The ethanol was evaporated to dryness, the solid was taken up in H_2O , and the mixture was filtered to remove unreacted ligand; a saturated solution of NH_4PF_6 was added to the filtrate, and the resulting orange precipitate was collected, dried, and chromatographed on neutral alumina (Alcoa F-20) using toluene: CH_3CN (1:2) as eluent. The first orange band off the column is the monometallic complex. The orange fraction was concentrated and precipitated by dropwise addition of the acetonitrile solution to rapidly stirred diethyl ether.

General Synthesis of $\{[(\text{dmb})_2\text{Ru}]_2(\text{b-b})\}(\text{PF}_6)_4$. A solution of $[(\text{dmb})_2\text{RuCl}_2]$ (1 equiv) and b-b (0.4 equiv) in ethanol was refluxed under N_2 for 5 h. The ethanol was evaporated to dryness, the solid was taken up in H_2O , and the mixture was filtered to remove unreacted ligand and the cis chloro complex; a saturated solution of NH_4PF_6 was added to this solution, and the resulting orange precipitate was collected, dried, and chromatographed on acidic alumina (EM Reagents) using CH_3CN as eluent. The monometallic complex remains at the top of the column, and the bimetallic complex is the first orange band off the column. Concentration and precipitation from diethyl ether was as above.

$[(\text{dmb})_2\text{Ru}(\text{bbdb})](\text{PF}_6)_2$ was prepared from 116 mg (2.15×10^{-4} M) of $[(\text{dmb})_2\text{RuCl}_2]$ and 594 mg (1.52×10^{-3} M) of **bbdb** ligand

using the above procedure. Yield: 176 mg (71%). FAB/MS (m/z): 1149.97 (M), 1005.3 (M - PF_6), 859.3 (M - 2 PF_6). Anal. Calcd for $\text{C}_{50}\text{H}_{46}\text{N}_8\text{RuP}_2\text{F}_{12}\cdot\text{H}_2\text{O}$: C, 51.42; H, 4.14; N, 9.59. Found: C, 51.43; H, 4.18; N, 8.98.

$\{[(\text{dmb})_2\text{Ru}]_2(\text{bbdb})\}(\text{PF}_6)_4$ was prepared from 414 mg (7.69×10^{-4} mol) of $[(\text{dmb})_2\text{RuCl}_2]$ and 100 mg (2.56×10^{-4} M) of **bbdb** ligand using the above procedure. Yield: 197 mg (40%). FAB/MS (m/z): 1909.45 (M), 1765.6 (M - PF_6), 1620.6 (M - 2 PF_6). Anal. Calcd for $\text{C}_{74}\text{H}_{70}\text{N}_{12}\text{Ru}_2\text{P}_4\text{F}_{24}$: C, 46.50; H, 3.70; N, 8.80. Found: C, 47.6; H, 4.59; N, 7.50.

$(\text{dmb})_2\text{Ru}(\text{bchb})](\text{PF}_6)_2$ was prepared from 158 mg (2.90×10^{-4} mol) of $[(\text{dmb})_2\text{RuCl}_2]$ and 820 mg (1.46×10^{-3} mol) of **bchb** using the above procedure. Yield: 135 mg. FAB/MS (m/z): 1322.15 (M), 1177.15 (M - PF_6), 1032.15 (M - 2 PF_6). The complex was used without further purification to make the bimetallic complex.

$\{[(\text{dmb})_2\text{Ru}]_2(\text{bchb})\}(\text{PF}_6)_4$ was prepared from 287 mg (5.33×10^{-4} mol) of $[(\text{dmb})_2\text{RuCl}_2]$ and 100 mg (1.78×10^{-4} mol) of **bchb** using the above procedure. Yield: 135 mg (36%). FAB/MS (m/z): 2082 (M), 1936 (M - PF_6), 1791.6 (M - 2 PF_6). Anal. Calcd for $\text{C}_{82}\text{H}_{82}\text{N}_{12}\text{O}_4\text{Ru}_2\text{P}_4\text{F}_{24}\cdot 4\text{H}_2\text{O}$: C, 45.73; H, 4.21; N, 7.80. Found: C, 45.69; H, 4.44; N, 7.38.

$(\text{dmb})_2\text{Ru}(\text{bphb})](\text{PF}_6)_2$ was prepared from 100 mg (1.85×10^{-4} M) of $[(\text{dmb})_2\text{RuCl}_2]$ and 380 mg (6.26×10^{-4} M) of **bphb** ligand using the above procedure. Yield: 156 mg (72%). FAB/MS: 1173.99 (M), 1029.3 (M - PF_6), (M - 2 PF_6), 698.3 [M - 2 PF_6 + dmb]. Anal. Calcd for $\text{C}_{52}\text{H}_{46}\text{N}_8\text{RuP}_2\text{F}_{12}\cdot 4\text{H}_2\text{O}$: C, 50.86; H, 4.27; N, 9.12. Found: C, 50.46; H, 4.16; N, 8.54.

$\{[(\text{dmb})_2\text{Ru}]_2(\text{bphb})\}(\text{PF}_6)_4$ was prepared from 269 mg (4.98×10^{-4} M) of $[(\text{dmb})_2\text{RuCl}_2]$ and 69 mg (1.67×10^{-4} M) of **bphb** ligand using the above procedure described elsewhere.²⁵ Yield: 150 mg (47%). FAB/MS (m/z): 1933.4 (M), 1789.29 (M - PF_6), 1643.5 (M - 2 PF_6). Anal. Calcd for $\text{C}_{76}\text{H}_{70}\text{N}_{12}\text{O}_4\text{Ru}_2\text{P}_4\text{F}_{24}\cdot\text{H}_2\text{O}$: C, 46.78; H, 3.72; N, 8.61. Found: C, 47.33; H, 4.16; N, 8.19.

Results

Ligand and Complex Syntheses. The bridging ligands **bbdb** and **bphb** were prepared as shown in Scheme 1. The NBS bromination of dmb has been reported before;²⁸ the reaction suffers from self-quaternarization as a significant side reaction. The phosphonium salt, prepared from the crude bromomethyl-

Table 1. Reduction Potentials of Compounds Examined in CH₃CN^a

compd	E_1, V ($\Delta E_p, n$)	E_2, V	E_3, V	E_4, V
[(dmb) ₃ Ru] ³⁺	1.14 (60, 1)	-1.41	-1.59	-1.82
bbdb		-1.51 (60)	-1.63 (irr)	
[(dmb) ₂ Ru(bbdb)] ³⁺	1.15 (60, 1)	-1.16 (60)	-1.51	-1.81
{[(dmb) ₂ Ru] ₂ (bbdb)} ⁶⁺	1.14 (60, 2)	-1.05 (60)	-1.16 (50)	-1.57 (90)
[(dmb) ₂ Ru(bchb)] ³⁺	1.16 (70, 1)	-1.36 (70)	-1.57 (80)	-1.80 (80)
{[(dmb) ₂ Ru] ₂ (bchb)} ⁶⁺	1.13 (70, 2)	-1.37 (70)	-1.59 (80)	-1.82 (80)
bphb		-1.78 (70)		
{[(dmb) ₂ Ru(bphb)] ³⁺	1.16 (80, 1)	-1.32 (80)	-1.55 (100)	-1.77
{[(dmb) ₂ Ru] ₂ (bphb)} ⁶⁺	1.13 (70, 2)	-1.28 (40)	-1.40 (50)	-1.58 (110)

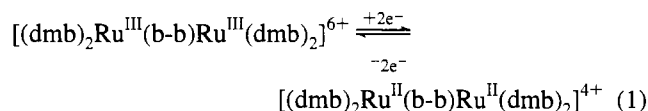
^a Potentials vs SSCE were obtained by cyclic voltammetry (100 mV/s) or differential pulse polarography (5 mV/s, pulse height = 20 mV) in CH₃CN containing 0.1 M tetraethylammonium perchlorate.

bipyridine, precipitates from the reaction mixture and can be used directly in the reaction with glyoxal trimeric dihydrate to yield the butadiene derivative (**bbdb**). Other glyoxal derivatives, such as the bisulfite addition product, do not react with the bipyridine ylide. Reaction of **bbdb** with dienophiles only yields product upon refluxing in neat diethyl fumarate. No reaction occurs with (dicarboxyethyl)acetylene in benzene or maleic anhydride in benzene. Decarboxylation and aromatization of the resulting cyclohexenyl-bridged bis(bipyridine) (**bchb**) to product **bphb** is most effective with Pb(OAc)₄; however some **bphb** is also obtained using Pd/C in acetone at high temperatures (250–300 °C). More recently we have devised a much more efficient route for preparing a derivative of **bphb** without the methyl groups.⁴¹

The complexes were prepared using methods essentially the same as those reported earlier for other complexes having one or two metal centers attached to the bridging ligand.⁴ The bridged metal dimers were chromatographed on acidic alumina to remove traces of the monomeric complexes which irreversibly adsorb to the alumina. The complexes were characterized by FAB mass spectrometry, spectrophotometry, cyclic voltammetry, and elemental analysis. All of the monometallic complexes gave FAB results for the highest mass cluster in good agreement with calculated spectra for the {[(dmb)₂Ru(BL)]PF₆}⁺ ions. The bimetallic complexes all showed intensity in the FAB spectra for ions having the formula {[(dmb)₂Ru]₂(BL)(PF₆)₃}⁺, although the experimental and calculated mass distributions were poor for the **bbdb** and **bphb** complexes. All of the complexes exhibited very low volatility and relatively weak FAB signals. Elemental analysis of {[(dmb)₂Ru]₂(bbdb)}(PF₆)₄ was less than satisfactory; the analysis was repeated on two independent samples purified by preparative TLC on alumina plates. While the analytical data are not exact, the impurities are not likely to

be Ru(II) diimine complexes since cyclic voltammograms and differential pulse polarograms show only a single Ru(III/II) wave.

Electrochemistry. Reduction potentials for the complexes and ligands in CH₃CN were obtained by cyclic voltammetry and differential pulse polarography. Results are shown in Table 1. The number of electrons involved in the first reduction listed in the Table is 1 for all the monometallic complexes and 2 for the bimetallic complexes; these values were determined by controlled potential electrolysis to within 10 %. Thus the initial reduction of the bimetallic complexes corresponds to reduction of both metal centers of the complex (eq 1). The E_1 values for



all three bimetallic complexes are more negative than the monometallic complexes having the same bridging ligand; this is somewhat unusual since the increased charge on the bimetallic complexes would be expected to slightly increase the E_1 values. The remaining potentials of Table 1 represent reduction of the coordinated diimine ligands. The first reductions of the complexes of **bphb** and **bbdb** occur at potentials positive relative to [Ru(bpy)₃]²⁺, indicating localization on the bridging ligand (*vide infra*).

Absorption and Luminescence Spectra. Absorption spectra were obtained in CH₃CN for all complexes at room temperature, and visible maxima are reported in Table 2. Spectra of **bbdb**, **bphb**, and the mono- and bimetallic complexes of these ligands are shown in Figure 2. In complexes having aliphatic tethers between linked bipyridines and in the **bchb**- and **bphb**-bridged complexes, little difference is observed in the absorption maximum between mono- and bimetallic complexes; however, the molar absorptivity of the bimetallic complexes is more than twice that of the monometallic complexes. In the **bbdb** bridged complexes, a 28 nm difference in the absorption maximum is observed between the mono- and bimetallic complexes and the molar absorptivity at the maximum is virtually the same for monometallic and bimetallic complexes.

Corrected emission spectra were obtained in room temperature acetonitrile. Emission maxima, quantum yields relative to [Ru(bpy)₃](PF₆)₂ in acetonitrile, and lifetimes in deaerated solutions are reported in Table 2. Room temperature emission of all the complexes is broad and lacks vibrational structure. Emission maxima and lifetimes were also obtained in 4:1 ethanol:methanol at 77 K, and results are reported in Table 2. The emission spectra exhibit vibrational structure in frozen solutions, and luminescence lifetimes increase by a factor of 4–5.

Table 2. Spectroscopic Properties of Complexes Examined

compd	λ_{max}, nm (log ϵ)	λ_{max}^{em}, nm (298 K)	λ_{max}^{em}, nm (77 K)	Φ_{em} (298 K)	τ_{em}, ns (298 K)	τ_{em}, ns (77 K)	τ_{TA}, ns (298 K)	$\eta_{isc}k_f$ s^{-1} (298 K)
[(dmb) ₃ Ru] ²⁺	460 (4.15)	616	589 640	0.086	770	4200	800	1.1×10^5
[(dmb) ₂ Ru(bbdb)] ²⁺	468 (4.16)	641	596 643	0.007	1040	4790	1370	6700
{[(dmb) ₂ Ru] ₂ (bbdb)} ⁴⁺	496 (4.26)	780		<0.001			540	
[(dmb) ₂ Ru(bchb)] ²⁺	458 (4.06)	623	592 646	0.098	1090	4550		9.0×10^4
{[(dmb) ₂ Ru] ₂ (bchb)} ⁴⁺	460 (4.41)	628	593 645	0.092	1060	4610		8.6×10^4
[(dmb) ₂ Ru(bphb)] ²⁺	466 (4.11)	632	605 649	0.109	1340	5140	1200	8.1×10^4
{[(dmb) ₂ Ru] ₂ (bphb)} ⁴⁺	468 (4.50)	641	613 664	0.125	1570	5090	1600	7.9×10^4

^a Samples were degassed with N₂ in MeCN for 5 min. ^b Lifetimes measured from TA at 550 nm.

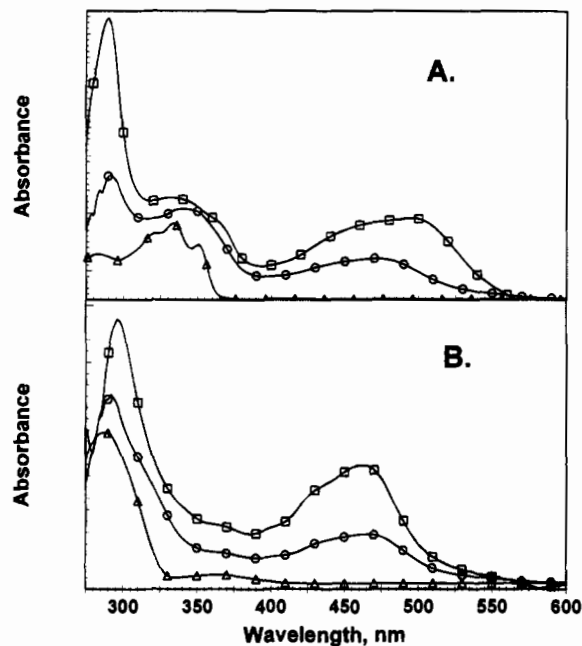


Figure 2. Room temperature absorption spectra of (A) **bddb** ($-\Delta-$), $[(dmb)_2Ru(bddb)](PF_6)_2$ ($-\circ-$), and $\{[(dmb)_2Ru]_2(bddb)\}(PF_6)_4$ ($-\square-$) and (B) **bphb** ($-\Delta-$), $[(dmb)_2Ru(bphb)](PF_6)_2$ ($-\circ-$), and $\{[(dmb)_2Ru]_2(bphb)\}(PF_6)_4$ ($-\square-$). Spectra are displayed to minimize overlap for clarity.

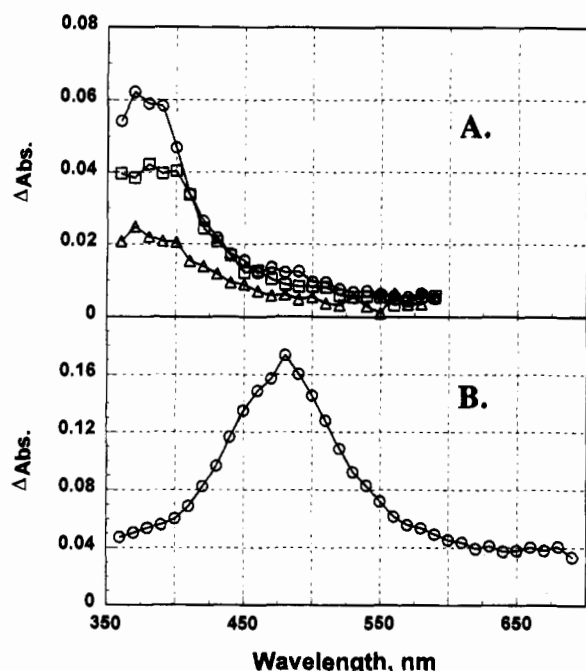


Figure 3. Transient absorption spectra of CH_3CN solutions of **bddb** (A) at 1.1 μs ($-\circ-$), 2.3 μs ($-\square-$), and 4.5 μs ($-\Delta-$) following excitation and **bphb** (B) at 1.5 μs following excitation at 308 nm (XeCl excimer).

Transient Absorption Spectra. Excited state absorption spectra of **bddb**, **bphb**, and all the complexes were obtained in room temperature acetonitrile. Figure 3 shows absorption spectra of the free ligands **bddb** and **bphb**, and Figures 4 and 5 show spectra of the monometallic and bimetallic complexes of **bddb** and **bphb**, respectively, at several times following excitation. The transient absorption spectrum of $[(dmb)_3Ru]^{2+}$ is also reported in Figure 4. For $[(dmb)_2Ru(bddb)]^{2+}$ quenching of transient absorbance and luminescence was examined for a series of triplet energy quenchers. Stern–Volmer quenching constants were determined for each quencher by examining the decrease in the lifetime of the transient absorption at 550 nm

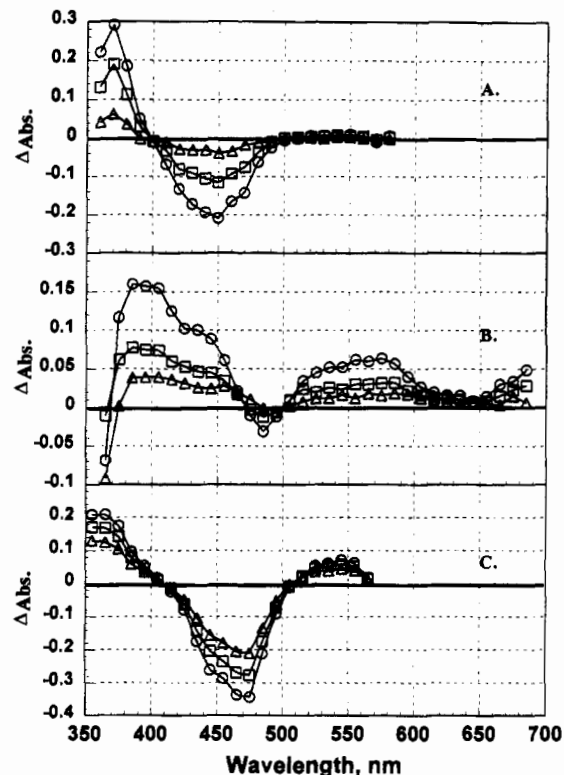


Figure 4. Transient absorption spectra in CH_3CN following dye laser excitation (460 nm) of $[(dmb)_3Ru](PF_6)_2$ (A) at 500 ($-\circ-$), 900 ($-\square-$), and 1500 ($-\Delta-$) ns following excitation, $[(dmb)_2Ru(bddb)](PF_6)_2$ (B) at 400 ($-\circ-$), 1600 ($-\square-$), and 2000 ($-\Delta-$) ns following excitation, and $[(dmb)_2Ru(bphb)](PF_6)_2$ (C) at 400 ($-\circ-$), 700 ($-\square-$), and 1000 ($-\Delta-$) ns following excitation.

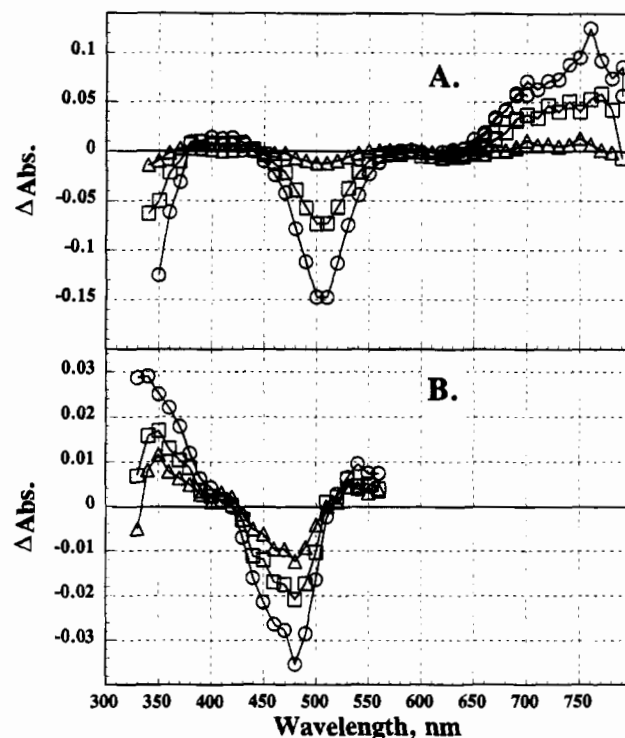


Figure 5. Transient absorption spectra in CH_3CN following dye laser excitation at 460 nm of $\{[(dmb)_2Ru]_2(bddb)\}(PF_6)_4$ (A) at 300 ($-\circ-$), 600 ($-\square-$), and 1500 ($-\Delta-$) ns following excitation and $\{[(dmb)_2Ru]_2(bphb)\}(PF_6)_4$ (B) at 400 ($-\circ-$), 1400 ($-\square-$), and 2000 ($-\Delta-$) ns following excitation.

and the luminescence of the complexes. Quenching rate constants are given in Table 3, and a plot of $\log(k_q)$ vs quencher

Table 3. Luminescence and Transient Absorbance Quenching of $[(\text{dmb})_2\text{Ru}(\text{bbdb})]^{2+}$ by Triplet Quenchers in CH_3CN

quencher	E_T, cm^{-1}	$10^{-8}k_q^{\text{em}},^a \text{M}^{-1} \text{cm}^{-1}$	$10^{-8}k_q^{\text{TA}},^b \text{M}^{-1} \text{cm}^{-1}$
phenazine	15 400	51.9	
anthracene	15 000	108	0.60
1-chloroanthracene	14 750	61	1.03
9,10-diphenylanthracene	14 500	35	2.6
9,10-dichloroanthracene	14 150	59	43
perylene	12 300	88	62

^a Quenching of 640 nm complex luminescence. Excitation wavelength = 460 nm. ^b Quenching of transient absorbance at 550 nm.

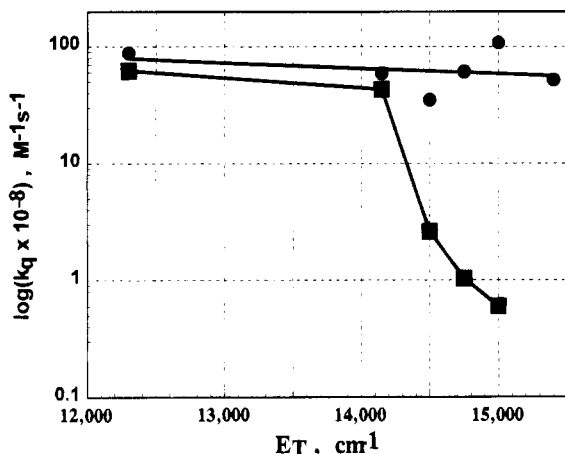
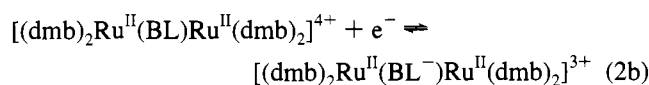


Figure 6. Rate constants for quenching of $[(\text{dmb})_2\text{Ru}(\text{bbdb})](\text{PF}_6)_2$ by a series of triplet quenchers as a function of the triplet energy of the quencher, E_T . Solid circles are for quenching of luminescence at 640 nm, and solid squares are for quenching of transient absorbance at 550 nm.

triplet energies is shown in Figure 6. The fact that the quencher triplet energy dependence of the quenching rate constant differs for the luminescence and transient absorbance suggests that the emitting state and the state having the transient absorbance at 550 nm are different.

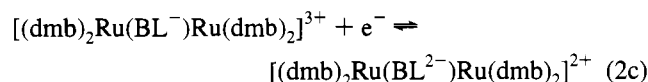
Discussion

a. Redox Properties. The relative degree of perturbation of the bridging ligand π^* level between coordination of one and two metals may be qualitatively assessed from the change in the bridging ligand localized reduction. The E_2 , E_3 , and E_4 values of Table 1 represent ligand-localized reduction. The first ligand-localized reduction, E_2 , of all the complexes can be assigned as being bridging ligand (BL) localized since reduction occurs at potentials at least 40 mV positive relative to the first ligand-localized reduction of $[\text{Ru}(\text{dmb})_3]^{2+}$ (eqs 2a,b). As can

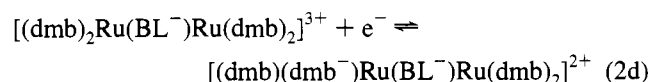


be seen in Table 1, the **bchb** reduction is essentially unchanged by coordination of a second Ru while the **bphb**- and **bbdb**-localized reductions become more positive by 40 and 110 mV, respectively. The anodic shift observed for complexes of all three ligands is relatively small when compared to complexes of 2,3-dipyridylpyrazine and other bridged dimers.^{29,30} The results suggest that **bchb** consists of localized π^* systems on each bipyridine while **bphb** and **bbdb** show increasing interaction of the linked bipyridines.

The second ligand-localized reduction, E_3 , can be either bridging ligand or dmb localized. The second reduction of the ligand **bbdb**, E_3 , occurs at a potential only 110 mV more negative than E_2 . Since the second reduction of the bimetallic complex of **bbdb** is positive relative to the first reduction of $[\text{Ru}(\text{dmb})_3]^{2+}$, E_3 is very likely also localized on the bridging ligand (eq 2c) in the bimetallic complex. Assignment of E_3

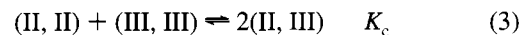


for the monometallic complex of **bbdb** and the bimetallic complex of **bphb** is less clear. In both complexes bridging ligand and dmb localized reductions (eq 2d) are reasonable. For



$[(\text{dmb})_2\text{Ru}(\text{bbdb}^-)]^+$ the observed difference between first and second reductions is 350 mV while that for the free ligand is only 120 mV; the asymmetry introduced in **bbdb** in the monometallic complex should increase the gap between the first and second ligand-localized reductions of **bbdb**, and it is not clear whether the second observed reduction is dmb or **bbdb** localized. Results for complexes having more strongly coupled conjugated bis-bidentate bridging ligands show that coordination of a second metal shifts both the first and second BL reductions to more positive potentials and that the potential difference $E_2 - E_3$ does not change significantly between monometallic and bimetallic complexes.^{30b} The **bbdb** complexes may differ from others reported since large geometric changes of **bbdb** are possible following reduction. The same analysis for the bimetallic complex of the **bphb** ligand was not possible since the second free ligand reduction was outside the potential window accessible.

Potentials for metal-centered reductions, Ru(III/II), are given by E_1 in Table 1. In complexes having two metal centers with identical coordination environments linked by a bridging ligand, the shape of the current-voltage profile in differential pulse polarography can provide a measure of the comproportionation equilibrium constant, K_c (eq 3).³¹ When reduction of one metal



does not perturb the second metal (localized charge), K_c is simply the statistical value and both metals are oxidized at the same potential. All three bimetallic complexes exhibit a single, unperturbed wave in both cyclic voltammetry and differential pulse polarography. The absence of broadening in differential pulse polarograms merely indicates that the interaction between the metal centers is not strong ($\leq 300 \text{ cm}^{-1}$).

b. Absorption Spectra. The absorption spectra of complexes having polyunsaturated bridging ligands represent a composite of intraligand ($\pi \rightarrow \pi^*$), metal to bridging ligand charge transfer (MLCT) and other charge transfer transitions. Figure 2 illustrates the relative contribution of intraligand absorption to the spectra of the mono- and bimetallic complexes. The lowest energy absorption in the complexes is MLCT and represents overlapping $\text{Ru}(d\pi) \rightarrow \text{BL}(\pi^*)$ and $\text{Ru}(d\pi) \rightarrow \text{dmb}(\pi^*)$ transitions. It is now well established that the energy of the lowest energy MLCT transitions is, for a related class of ligands, linearly related to the difference between the first one electron reduction and the first one electron oxidation potentials (ΔE). In all of the complexes reported here the Ru(III/II) potential is nearly the same and the first reduction is localized

on the bridging ligand. As a result, the lowest energy MLCT transition is expected to be $\text{Ru}(\text{d}\pi) \rightarrow \text{BL}(\pi^*)$. The data of Tables 1 and 2 indicate that there is reasonable qualitative agreement between the MLCT maxima and ΔE . The absorption maximum of $[(\text{dmb})_2\text{Ru}]_2(\text{bbdb})^{4+}$ is nearly the same as that reported for the bimetallic complex $\{[(\text{bpy})_2\text{Ru}]_2(\text{bbpe})\}^{4+}$, where **bbpe** = *trans*-1,2-bis(4'-methyl-2,2'-bipyridin-4-yl)ethene ($\lambda_{\text{max}} = 500 \text{ nm}$).³² The lack of a red shift in the absorption maximum between **bbpe** and **bbdb** complexes is analogous to the near constancy in the MLCT absorption maxima observed for the series $[(\text{NH}_3)_x\text{Ru}(\text{py}(\text{CH}=\text{CH})_x\text{py})\text{Ru}(\text{NH}_3)_5]^{4+}$ ($x = 2-4$).⁴⁰

The molar extinction coefficients reported for the complexes do not follow any simple trend. In complexes having bis-bidentate bridging ligands with saturated tethers the molar absorptivities of the symmetric bimetallic complexes are simply twice that of the monometallic derivatives (i.e. $[(\text{bpy})_2\text{Ru}(\text{BL})]^{2+}$ vs $\{[(\text{bpy})_2\text{Ru}]_2(\text{BL})\}^{4+}$). In these complexes the visible absorption maxima reported represent the net maximum observed for overlapping $\text{BL}(\pi \rightarrow \pi^*)$, $\text{Ru}(\text{d}\pi) \rightarrow \text{BL}(\pi^*)$, and $\text{Ru}(\text{d}\pi) \rightarrow \text{dmb}(\pi^*)$ MLCT transitions. The energy of the $\text{Ru}(\text{d}\pi) \rightarrow \text{BL}(\pi^*)$ transition exhibits a bathochromic shift upon coordination of the second metal center; for the complexes of **bbdb**, the small increase in the molar extinction coefficient between the monometallic and bimetallic complexes is a result of a decrease in the overlap of the $\text{Ru}(\text{d}\pi) \rightarrow \text{bbdb}(\pi^*)$ and $\text{Ru}(\text{d}\pi) \rightarrow \text{dmb}(\pi^*)$ transitions. It is more difficult to explain the more than 2-fold increase in the molar absorptivity of the observed MLCT transitions of $[(\text{dmb})_2\text{Ru}(\text{bphb})]^{2+}$ and $\{[(\text{dmb})_2\text{Ru}]_2(\text{bphb})\}^{4+}$; this behavior is also observed in complexes of **bdvbb** (*vide supra*).^{22b} One possibility is that the $\text{Ru}(\text{d}\pi) \rightarrow \text{bphb}(\pi^*)$ transition dipole is larger in the bimetallic complex than in the monometallic complex. Clearly the transition dipole length is important in influencing the molar absorptivity in complexes having MLCT transitions. For example, the complex $[\text{Ru}(\text{dmb})_3]^{2+}$ has an ϵ value of $14\,000 \text{ M}^{-1} \text{ cm}^{-1}$ while that of $[\text{Ru}(\text{styb})_3]^{2+}$ (styb = 4,4'-distyryl-2,2'-bipyridine) is $33\,000 \text{ M}^{-1} \text{ cm}^{-1}$.^{22b}

c. Photophysical Behavior. The complexes having the ligands **bphb** and **bchb** have luminescence maxima between 620 and 640 nm, luminescence quantum yields between 0.09 and 0.03, and radiative decay rate constants around $8 \times 10^4 \text{ s}^{-1}$. Table 2 shows that the luminescence lifetimes, emission quantum yields, and radiative decay constants are very similar for the two complexes of each ligand. A slight bathochromic shift in the emission maximum is observed upon adding the second metal center to **bphb**. The redox data indicate a smaller difference between E_1 and E_2 for the bimetallic complex of **bphb** which is consistent with the observation of a lower energy emission maximum.^{33a} An interesting feature of the **bphb** complexes is that their luminescence lifetimes are nearly twice that of $[\text{Ru}(\text{dmb})_3]^{2+}$ even though the emission occurs at lower energy. Extensive investigations of Meyer and co-workers have shown that, for series of closely related complexes having ³MLCT excited states, the nonradiative decay rate constant increases as the energy gap decreases (decay follows Golden rule behavior).³³ Between different series of complexes the relative rate constants for excited state relaxation are inversely related to the comparative degree of distortion of the excited state relative to the ground state in each series. Meyer attributed the long-lived luminescence of $\{[(\text{dmb})_2\text{Ru}]_2(\text{bbpe})\}^{4+}$ to a smaller degree of excited state distortion (smaller electron-vibronal coupling constant) relative to Ru(II) diimine complexes having similar emission energies. The smaller distortion is presumably due to greater delocalization of the

excited electron in the **bbpe** π^* network relative to other diimine ligands. Experimental evidence for this can be obtained from fits of 77 K emission spectra; the relative intensities of the first two vibronic bands are directly affected by the degree of electron-vibronal coupling. The complexes of **bphb** also have low-temperature luminescence spectra which indicate a smaller degree of excited state distortion than $[\text{Ru}(\text{dmb})_3](\text{PF}_6)_2$, a complex having a comparable emission maximum. Thus these complexes provide another example of this effect, which is desirable in the development of efficient sensitizers having MLCT excited states. We are currently examining this in more detail for other complexes of **bphb** and for complexes having two or more phenyl spacers between covalently linked bipyridines.

The **bbdb** complexes exhibit extremely weak luminescence, and the experimental radiative decay rate constant of the monometallic complex (Table 2) is very low. Thorough experimentation with Ru(II) diimine complexes has shown that radiative decay rate constants for ³MLCT states are, without exception, greater than 10^4 s^{-1} . The observed radiative decay rate constant includes the intersystem crossing efficiency to populate the ³MLCT state (Figure 1), $k_{\text{r,obs}} = \eta_{\text{isc}}k_{\text{r}}$. Thus, an observed k_{r} lower than 10^4 s^{-1} , like that for the monometallic complex of **bbdb**, implies either rapid relaxation of the ¹MLCT state back to the ground state or formation of another state. Intersystem crossing from the ¹MLCT state to the ³MLCT state in Ru(II) diimine complexes is known to be highly efficient.⁴⁴ While a diminished intersystem crossing efficiency cannot be dismissed for the monometallic **bbdb** complex, we presently have no basis for asserting this explanation; however, combined results from transient absorbance and luminescence studies confirm the existence of two separate transient species following excitation (*vide infra*).

Both complexes of **bbdb** have unique transient absorbance throughout the visible with lifetimes between 500 ns and $1 \mu\text{s}$ in freeze-pump-thaw degassed solutions (Figures 4 and 5). The transient spectra of the **bbdb** complexes exhibit bleaching at wavelengths to the blue of 360 nm which reflects bleaching of the strongly absorbing **bbdb** $\pi \rightarrow \pi^*$ transition of the ground state, a second bleaching associated with the MLCT absorption between 450 and 520 nm, and a strong absorbance in the red. The monometallic complex exhibits single exponential decays of transient absorption at both 400 and 550 nm. Also, the transient spectrum of the monometallic **bbdb** complex is not changed when the solvent is changed from CH_3CN to CH_2Cl_2 or ethanol. The transient absorbance of the monometallic complex at 550 nm is nearly completely quenched by O_2 ($\tau < 20 \text{ ns}$) in CH_3CN . In addition, the transient absorbance is efficiently quenched by triplet quenchers having triplet state energies lower than $14\,500 \text{ cm}^{-1}$ (Table 3) while the luminescence is quenched at near-diffusion-limited rates with quenchers having triplet states as high as $15\,000 \text{ cm}^{-1}$. If it is assumed that the activation barrier for exchange energy transfer is low for quenching of the excited state giving rise to the transient absorbance of the **bbdb** complexes, the quenching rate constant will be expected to become diffusion limited when the free energy for the process is nearly zero. While the data are limited, Figure 6 shows that the diffusion limit for quenching of the transient of $[(\text{dmb})_2\text{Ru}(\text{bbdb})]^{2+}$ is reached with quenchers having triplet excited states of approximately $14\,000 \text{ cm}^{-1}$. The difference in quenching of the luminescence and the transient absorbance provides clear evidence for the existence of two

(44) (a) Demas, J. N.; Taylor, D. G. *Inorg. Chem.* **1979**, *18*, 3177. (b) Mandal, K.; Pearson, T. D. L.; Krug, W. P.; Demas, J. N. *J. Am. Chem. Soc.* **1983**, *105*, 701.

long-lived excited states. While the transient absorption spectrum of the monometallic **bbdb** complex should represent the combined absorption of both the $^3\text{MLCT}$ and a second state, the absorption of the second state could dominate over that of the $^3\text{MLCT}$ state if intersystem crossing to the state is highly favored. If a radiative decay rate constant of $5 \times 10^4 \text{ s}^{-1}$ is assumed for the $^3\text{MLCT}$ state, the intersystem crossing efficiency to the $^3\text{MLCT}$ state would be 0.13 (since $k_r\eta_{isc} = 6700 \text{ s}^{-1}$) and the maximum yield of the second state would be 0.87.

The bimetallic complex $\{[(\text{dmb})_2\text{Ru}]_2(\text{bbdb})\}^{4+}$ exhibits extremely weak luminescence with a maximum of approximately 750 nm ($13\,300 \text{ cm}^{-1}$). The complex also has a rich transient absorbance with strong absorbance in the red (Figure 5); the decay of this transient is single exponential. Qualitative transient absorbance quenching results for the complex indicate that the free energy dependence is similar to that observed for the monometallic complex. In this case the energy of the emitting state is lower than the energy of the state giving rise to the transient absorbance. In addition, the lifetime of the transient absorbance is shorter than that observed for the monometallic complex.

The transient formed in addition to the luminescent $^3\text{MLCT}$ state may involve generation of a ligand-localized triplet state, exciplex formation (with the solvent or an anion), or creation of a twisted intramolecular charge transfer (TICT) state. Considerable work has focused on the formation of exciplexes involving transition metal complex chromophores. McMillin has reported and characterized exciplexes of Cu(I) phenanthroline complexes with various Lewis bases in organic solvents; the exciplex is believed to involve expansion of the coordination sphere of the Cu(I).⁴⁵ In addition, Watts has recently provided evidence for exciplexes of Ir(III) 8-quinolyldiphenylsilyl complexes with solvents.⁴⁶ Solvents which act as σ donors form exciplexes via binding at the metal center while π acceptor solvents (i.e. olefins and aromatic hydrocarbons) bind at the quinolyl anion radical site associated with the σ -bond-to-ligand charge transfer state. In cases of solvent exciplex formation the emission lifetime of the chromophore is dependent on the nature of the particular solvent and the mole fraction of complexing solvent in an inert solvent. The similarity of results from transient absorbance studies of the monometallic **bbdb** complex in three solvents suggests exciplex formation is not likely.

TICT states are sometimes observed in substances for which twisting about a molecular axis stabilizes a particular charge transfer state relative to other states in any conformation.⁴⁷ Such states are most commonly observed for organic chromophores having clearly defined donor and acceptor moieties such as aromatic amines/anilines. However, unsubstituted biaryl compounds are known to have luminescent TICT states. The energy of the TICT state can be approximated from the ionization potential of the donor, electron affinity of the acceptor, the solvation energy of the ion pair, and the Coulombic attraction of the donor and acceptor pair. This is essentially the same as the formalism for determining the energy of a MLCT state. The question that arises then is whether or not twisting of the initially formed $^3\text{MLCT}$ state of the **bbdb** complex will result in a stabilized TICT state. Regardless of twisting, the excited state assignment is charge transfer in nature. In the complex $\{[(\text{dmb})_2\text{Ru}]_2(\text{bbpe})\}^{4+}$ (**bbpe** = 1,2-bis(4'-methyl-2,2'-bipyridin-4-yl)ethene) Meyer and co-workers assigned the transient

Table 4. Triplet Energies and Triplet-Triplet Absorption Maxima of Ligands and Related Aromatic Hydrocarbons

compd	$\lambda_{\text{max}}^{\text{TA}}$, nm	E_{T} , cm^{-1}
bphb	470	
<i>p</i> -terphenyl	460	20 200
bvinb ^a		
<i>t</i> -stilbene ³⁴	360	17 500
[Ru(dmb) ₃]	360	16 000
bdvbb	500	14 200
1,4-distyrylbenzene ³⁵	505	14 500
bbdb	370	14 100
1,4-diphenylbutadiene ³⁶	390	14 500

^a **bvinb** = 1,2-bis(4-methyl-2,2'-bipyridin-4-yl)-ethene.

absorbance in the red as being due to a bridging ligand localized absorption of the $^3\text{MLCT}$ state based upon analogy to spectra of pyridinium salts having low one electron reduction potentials.³² However, triplet excited states of organics having an olefin bridge between an aromatic ring and a quaternary aza-aromatic ring, such as *N*-alkyl-4-(4-styryl)quinolinium salts, have transient spectra similar to the mono- and bimetallic **bbpe** and **bbdb** complexes.³⁷ Thus, the absorption in these complexes can simply be assigned as a $\pi_1^* \rightarrow \pi_2^*$ transition of a ligand-localized excited state. In addition, evidence is accumulating that ^3IL excited state energies of aza-aromatic ligands are nearly the same as the triplet energies of the coordinated ligands. Results from several groups have shown that Re(I) complexes of substituted phenanthrolines and bipyridines have ^3IL phosphorescence at 77 K which has nearly the same energy and vibronic structure as the phosphorescence of the ligand alone.^{22,42,43} Since the **bbdb** ligand has an extended π network similar to 1,4-diphenylbutadiene (which has a triplet energy of approximately $14\,500 \text{ cm}^{-1}$)³⁶, the existence of a low-energy intraligand excited state is certainly possible.

d. Intraligand Excited States and Ligand Structure. The results here can be combined with other results in the literature³² to correlate bridging ligand structure and the presence of intraligand states (^3IL) in complexes having lowest energy MLCT absorption. Transient absorption spectra of the ligands **bdvbb**, **bbdb**, and **bphb** were found to be strikingly similar to spectra reported for the aromatic hydrocarbons 1,4-distyrylbenzene, 1,4-diphenylbutadiene, and *p*-terphenyl, respectively. Extensive work of Göerner and others has illustrated the similarity between aza-aromatic hydrocarbons and the parent hydrocarbons.³⁷ From triplet quenching studies (or direct ^3IL emission) we have determined approximate ^3IL state energies for **bdvbb** and **bbdb** coordinated to Ru(II). The energies obtained are nearly the same as those reported for closely related aromatic hydrocarbons (i.e. **bbdb** is close in energy to 1,4-diphenylbutadiene). Table 4 shows the correlation of transient absorption maxima of four bis(bipyridine) ligands and the triplet energies and excited state absorption spectral maxima of closely related hydrocarbons. While the data are very limited, the suggestion is that triplet energies of simple aromatic hydrocarbons may be used to predict approximate triplet energies of the structurally related bridging ligands and, thus, the degree of importance of ^3IL states in complexes where the $^3\text{MLCT}$ energy can be estimated.

The ligand **bphb** and others such as *bpy*, *dmb*, and *phen* have triplet energies above that of the approximate energy of the zero-zero level, E_{00} , of the $^1\text{MLCT}$ state of complexes containing these ligands. In such complexes, intersystem crossing from the $^1\text{MLCT}$ state to the ^3IL state of the ligand is energetically uphill and the observed behavior is consistent with efficient population of the $^3\text{MLCT}$ state. By contrast, the behavior of complexes of **bdvbb** and **bbdb**, and to a lesser

(45) (a) Stacy, E. M.; McMillin, D. R. *Inorg. Chem.* **1990**, *29*, 393. (b) McMillin, D. R.; Kirchoff, J. R.; Goodwin, K. V. *Coord. Chem. Rev.* **1985**, *64*, 83.

(46) Djurovich, P. I.; Watts, R. J. *J. Phys. Chem.* **1994**, *98*, 396.

(47) Rettig, W. *Top. Curr. Chem.* **1994**, *169*, 253.

extent **bbpe**, strongly suggests the presence of ^3IL states. The IL states are observed even when they are higher in energy than the $^3\text{MLCT}$ state of the complex. Thus, while extended delocalization in ligands can lead to $^3\text{MLCT}$ states having long lifetimes, the possibility also exists to introduce ^3IL states which are populated competitively with $^3\text{MLCT}$ states. It is not clear what factors influence internal conversion between the two states formed upon intersystem crossing from the $^1\text{MLCT}$ state.

Summary

Results from this work and previous studies strongly suggest two excited triplet species can be formed following excitation into MLCT absorption bands of Ru(II) diimine complexes. The principal criterion is that the energy of the states being populated lies below the $^1\text{MLCT}$ state. In mono- and bimetallic complexes having polyunsaturated covalent links in bis(bipyridyl) ligands, the triplet energies of the bis(bipyridyl) ligands are close in energy to those of simple aromatic hydrocarbons having closely related skeletal frameworks. As a result, the likelihood of forming a ^3IL state following MLCT excitation of Ru(II)

complexes containing these ligands can be determined from the energies of the $^1\text{MLCT}$ state and the triplet state of the hydrocarbon paralleling the bridging ligand. Since bridging ligand unsaturation serves to enhance rate constants for photoinduced intramolecular energy and electron transfer reactions between adjacent metal centers, it is useful to predict possible ligand-localized states which may serve as energy traps.

Acknowledgments. This work was sponsored by the donors of Petroleum Research Fund, administered by the American Chemical Society, and by the Division of Chemical Sciences, Office of Basic Energy Sciences, Department of Energy, under Contract DE-FG05-92ER14309. The authors wish to thank Dr. Debbie Grimm of the Tulane Coordinated Instrumentation Facility for obtaining the mass spectra.

Supplementary Material Available: Figures showing FAB mass spectral data for the M-PF_6 ions of complexes of **bphb**, **bchb**, and **bbdb** (6 pages). Ordering information is given on any current masthead page.

IC931021F